Evolution of ZnO architecture on a nanoporous TiO_2 film by a hydrothermal method and the photoelectrochemical performance*

Jiang Yinhua(蒋银花)[1,2], Wu Xiaoli(吴小黎)[1], Zhang Wenli(张文莉)[1], Ni Liang(倪良)[1], and Sun Yueming(孙岳明)[2,†]

[1]School of Chemistry and Chemical Engineering, Jiangsu University, Zhenjiang 212013, China
[2]School of Chemistry and Chemical Engineering, Southeast University, Nanjing 211189, China

Abstract: The synthesis of ZnO architecture on a fluorine-doped SnO_2 (FTO) conducting glass pre-coated with nanoporous TiO_2 film has been achieved by a one-step hydrothermal method at a temperature of 70 ℃. The effect of the reaction time on the morphology of the ZnO architecture has been investigated, and a possible growth mechanism for the formation of the ZnO architecture is discussed in detail. The morphology and phase structures of the as-obtained composite films have been investigated by field-emission scanning electron microscopy (FE-SEM) and X-ray diffraction (XRD). The results show that the growth time greatly affects the morphology of the obtained ZnO architecture. The photoelectrochemical performances of as-prepared composite films are measured by assembling them into dye sensitized solar cells (DSSCs). The DSSC based on the as-prepared composite film (2 h) has obtained the best power conversion efficiency of 1.845%.

Key words: ZnO architecture; nanoporous TiO_2 film; hydrothermal synthesis; dye-sensitized solar cell
DOI: 10.1088/1674-4926/32/3/033005 **EEACC:** 2520

1. Introduction

ZnO, a wide band gap semiconductor with a large excitation binding energy, is one of the most promising functional materials due to its catalytic, electrical, optoelectronic, and piezo-electric properties. In recent years, ZnO nanoparticles or nanostructures have been widely used in gas sensors[1], luminescence[2], piezoelectric transducers and actuators[3], photocatalysts[4], and solar cells[5]. Very recently, aligned ZnO nanostructures (e.g., nanorods, nanowires, nanoneedles) directly grown on transparent substrates have become of interest and are intensively researched for their potential application in dye-sensitized solar cells (DSSCs) or semiconductor quantum dots sensitized solar cells (QDSSCs). For instance, Law *et al*.[6] has reported 1.2%–1.5% efficiency for the DSSC based on ZnO nanowire arrays of high surface area grown on FTO substrates using a seeded growth process. The direct electrical pathways provided by the nanowires improve electron transport by avoiding the particle-to-particle hopping that occurs in the TiO_2 network[7]. Sun *et al*.[8] has assembled a quantum dot sensitized solar cell (QDSSC) with power conversion efficiency of 0.45% based on the bilayer ZnO nanostructure, with a nanoflower on the upper layer and a nanorod array on the bottom layer grown by a chemical bath growth process on ITO glass. The bilayer ZnO assembled QDSSC has obtained a three times higher power conversion efficiency value than the ZnO nanorods array. The shape of the ZnO nanoflower can increase the adsorption intensity of sensitizers to improve the overall power conversion efficiency of the solar cell[9]. TiO_2, as another functional semiconductor, has been extensively investigated due to its relatively low toxicity, low cost, and resistance to photocorrosion[4]. It is the most used semiconductor in dye-sensitized solar cells[10−12]. So using TiO_2 thin film modified substrate to synthesize morphologically controllable ZnO architecture may be very significant in improving the performance of dye-sensitized solar cell. In this study, we report the synthesis of a two-layer ZnO architecture, with a flower-like microstructure on the top layer and nanorod arrays on the bottom layer on fluorine-doped SnO_2 (FTO) conducting glass pre-coated with a nanoporous TiO_2 film by a one-step hydrothermal process. The effects of hydrothermal time on the morphologies of the resultant products are systematically investigated. A possible growth mechanism is also proposed for this ZnO architecture. In addition, extensive DSSC studies are performed to determine the morphological effect on the photoperformance of the ZnO architecture.

2. Experimental

2.1. Materials

The following reagents were used: zinc nitrate hexahydrate ($Zn(NO_3)_2{\cdot}6H_2O$), ammonium hydroxide [NH_4OH (28%)], tetrabutylorthotitanate ($C_{16}H_{36}O_4Ti$), ethyl cellulose, nitric acid, alcohol and α-terpineol. All reagents were analytic grade and used without further purification. Distilled water was used throughout all of the experiments. Fluorine-doped SnO_2 (FTO, 10 Ω/cm^2) conducting glass plates were used as substrates and cleaned by standard procedures prior to use.

Nanoporous TiO_2 film on fluorine-doped SnO_2 (FTO) conducting glass was prepared by a screen-printing method. Screen printing TiO_2 paste was prepared by the following pro-

* Project supported by the National Basic Research Program of China (No. 2007CB936300) and the Research Foundation for Advanced Talents of Jiangsu University, China (No. 10JDG142).
† Corresponding author. Email: yms418@126.com
Received 1 September 2010, revised manuscript received 12 November 2010

cedure. 12.5 mL tetrabutylorthotitanate was added dropwise into 150 mL distilled water with a pH of 1.5. The pH of the distilled water was adjusted by nitric acid under vigorous stirring. The solution was continually stirred at room temperature for more than 10 h. Then, the solution was heated in an oil bath at 75 ℃ for 8 h under vigorous stirring. Sol samples obtained by hydrolysis reaction were transferred into a Teflon lined stainless steel autoclave. Hydrothermal reactions were conducted at 200 ℃ for 24 h. After hydrothermal reaction, the ivory-yellow gels were centrifuged, and then washed with distilled water and alcohol several times. The washed TiO_2 gels were added to the mixture solution of ethyl cellulose and α-terpineol with a weight ratio of TiO_2 : ethyl cellulose : α-terpineol of 73 : 9 : 18, then the mixture was continually stirred overnight until a homogeneous paste was obtained. Via a screen printing technique the paste was spread onto fluorine-doped SnO_2 conducting glass and was dried in air at 80 ℃ for 1 h. Then the substrate was sintered at 450 ℃ for 30 min and finally cooled to room temperature. A thin nanoporous TiO_2 film (1 μm) on fluorine-doped SnO_2 (FTO) conducting glass was prepared.

2.2. Composite film preparations

A ZnO coating layer was grown using a simple one-step hydrothermal process. In a typical experiment, 0.6 g $Zn(NO_3)_2{\cdot}6H_2O$ was added to 100 mL distilled water under magnetic stirring. Then ammonium hydroxide was added dropwise to the above solution under vigorous stirring until the pH of the solution was 10.8. The as-prepared solution was transferred into a Teflon-lined stainless steel autoclave, and fluorine-doped SnO_2 (FTO) conducting glasses pre-coated with nanoporous TiO_2 film were placed in the autoclave and kept level during the hydrothermal process. The tank was conducted in an electric oven at 70 ℃ for different reaction times. After the reaction, the obtained products were washed with distilled water and dried. A series of experiments showed that the growth time was a main factor in influencing the structural shapes of the ZnO structure grown on the nanoporous TiO_2 film.

2.3. Characterization

The morphology and structure of the products were characterized with field-emission scanning electron microscopy (FE-SEM, Philips FEI XL30) and X-ray diffraction (XRD, Rigaku D-max 2200, CuKα). To measure the photoelectrochemical property, the as-prepared ZnO-based film electrode was heated at 100 ℃ for 1 h, and then immersed into a 0.3 mM ruthenium (II) cis-di (thiocyano) bis (2,2'-bypyridyl-4,4'-dicarboxylic acid) (N3) dye/ethanol solution for 3 h. A simple sandwich cell was assembled by using a N3-sensitized ZnO-based film electrode with an active area of 0.5 cm^2 as the working electrode and a Pt-coated FTO was used as a counter electrode. A thin layer of electrolyte was introduced into the interelectrode space. The electrolyte was composed of 0.5M LiI, 0.05M I_2 and 0.5M 4-tertbutylpyridine (TBP) in a propylene carbonate. The photocurrent–photovoltage characteristics of the solar cells were measured by a Keithley model 2400 digital source meter using an Oriel 91192 solar simulator equipped with an AM 1.5 filter and an intensity of 100 mW/cm^2.

3. Results and discussion

3.1. Effect of growth time on the morphology of the ZnO coating layer

The hydrothermal growth time greatly influences the morphology of the ZnO coating layer grown on TiO_2 film, so synthetic experiments at different reaction time were carried out at 70 ℃ with a pH of 10.8. Figure 1 shows the FE-SEM images of the ZnO architecture grown for different reaction times. Figures 1(a) and 1(b) present low- and high-magnified FE-SEM images of the products with a reaction time of 30 min. From these FE-SEM images, ZnO structures can not be obviously found on the surface of the nanoporous TiO_2 film. However, the energy dispersive spectroscopy (EDS) of this product (Fig. 2) shows the presence of Zn and O, which indicates that the surface of the TiO_2 film is covered with ZnO nuclei nanoparticles after reaction for 30 min.

When the reaction is performed for 1 h, a small amount of white precipitate begins to form. As shown in Figs. 1(c) and 1(d), ZnO crystals have grown to small spindle-like ZnO nanorods with one side randomly oriented on the TiO_2 surface. The size of the spindle-like ZnO nanorod is in the range of 100–170 nm and the surface seems very rough. Meanwhile, new ZnO crystals are continuously formed as the reaction proceeds. After 1.5 h, from the low magnified FE-SEM image of the product (Fig. 1(e)), it can be observed that a dense ZnO nanorod array has formed on the surface of the TiO_2 film, but no flower-like ZnO structure can be found. The high-magnified FE-SEM image of the product (Fig. 1(f)) shows that the bottom part of the spindle-like nanorod has evolved into hexagonal pyramids with a smooth surface, but the top part still seems very rough. The typical diameters of these individual ZnO nanorods are in the range of 30–70 nm with a length of 400–700 nm.

When the reaction time is increased to 2 h, as shown in Fig. 1(g), a two-layer structure of ZnO architecture begins to form, with several flower-like ZnO microstructures dispersed on the top layer and a dense ZnO nanorod array grown on the bottom layer. Figure 1(g) clearly shows that an individual flower-like structure comprises three to ten hexagonal-pyramid nanopetals with smooth surfaces. The diameter of the petals varies from the base to the tips, showing that the petals have sharpened tips with the wider bases that are connected to each other through their wider bases. The diameters of these petals at their tips and bases are between 30–100 and 300–650 nm, respectively, and the lengths of these petals are 500 nm–2 μm. The full arrays of one flower-shaped structure are in the range of 3–5.5 μm. The FE-SEM image of nanorods grown on the bottom layer shows that nanorods have grown to large sizes in all orientations and covered the entire surface of the TiO_2 film (Fig. 1(h)). The typical diameters of these individual ZnO nanorods are in the range of 110–180 nm with a length of 500–1.2 μm. Additionally, the surface of the ZnO hexagonal nanorod is very smooth and well faceted. According to the evolution process of the surface of the ZnO, it is indicated that the crystallization of ZnO increases when the reaction time is increased. When the reaction time is further increased, the size and quantity of the flower-like ZnO structures obviously increase, and the density of the nanorod array also becomes

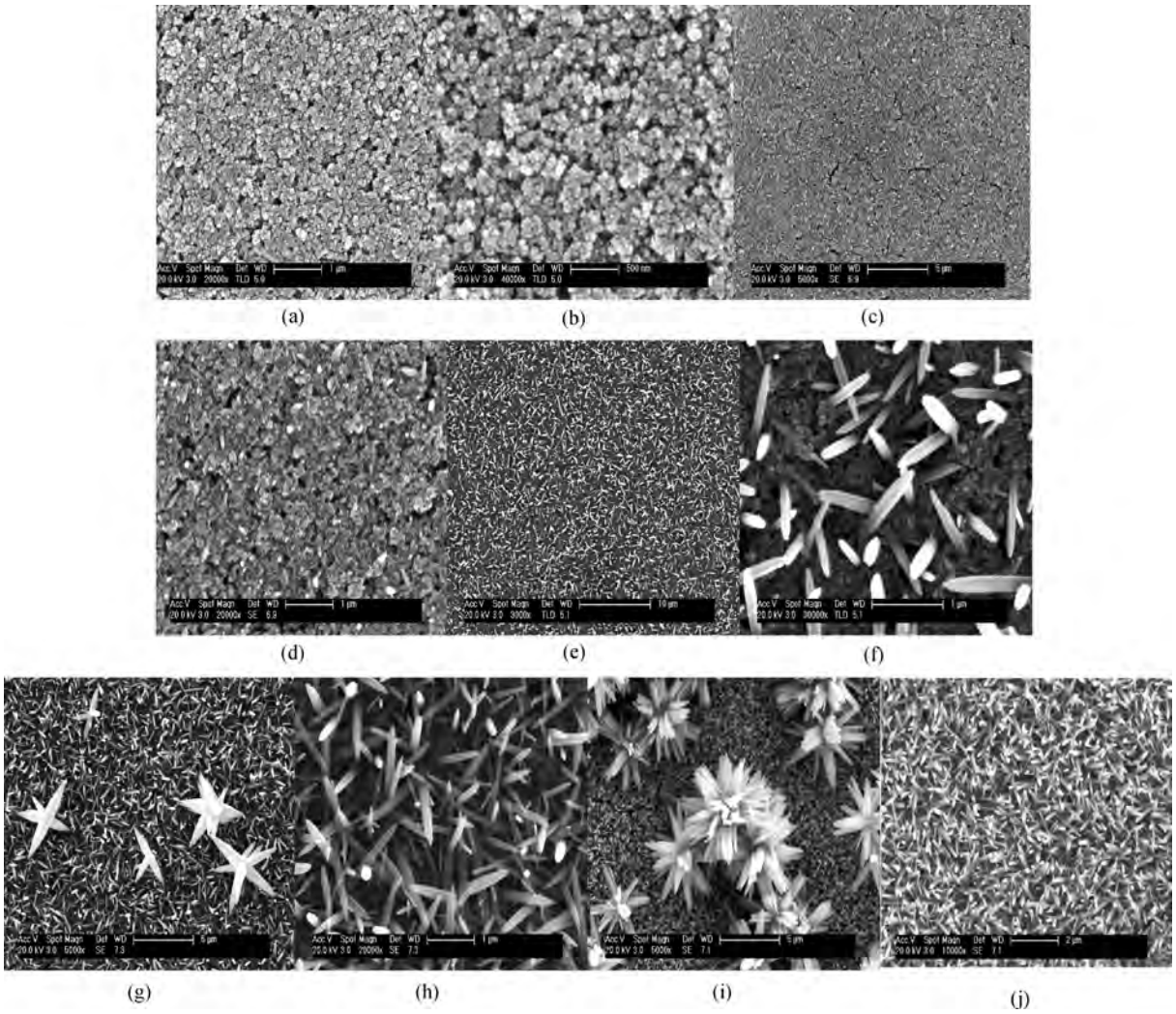

Fig. 1. (a, c, e, g, i) Low-magnified and (b, d, f, h, j) high-magnified FE-SEM images of architectures for the different growth times (top view). (a, b) 30 min. (c, d) 1 h. (e, f) 1.5 h. (g, h) 2 h . (i, j) 6 h.

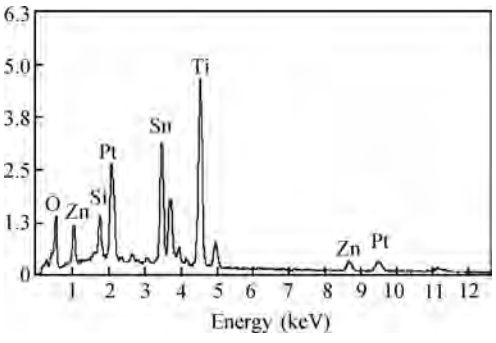

Fig. 2. Energy-dispersive X-ray spectrometer (EDS) analysis of the ZnO architecture for a growth time of 30 min.

greater, as shown in Figs. 1(i) and 1(j). From Fig. 1(i), it can be seen that the ZnO architecture grown on the nanoporous TiO_2 film has a two-layer structure, with flower-like ZnO microstructures on the top layer and ZnO nanorod arrays on the bottom layer. The flower-like ZnO microstructure with approximately uniform morphology is randomly dispersed on the top of the ZnO nanorod. The flower-shaped structures are constituted by the accumulation of several hundreds of plane-tipped hexagonal ZnO nanorods. The typical diameters of these individual nanorods are in the range of 100–700 nm with a length of 1.5–4 μm. The size of the full array of a flower-shaped structure is in the range of 6–9 μm. All of the nanorods radiate through the center to form 3D flower-like structures. In addition, the rod tip appeared plane with wide hexagonal-bases and the surfaces of the ZnO rods are very smooth. Figure 1(j) shows FE-SEM images of ZnO nanorods grown on the bottom layer at high magnification. It can be clearly seen that the ZnO nanorods are aligned in a high-density array over the entire surface of the TiO_2 film. Such a nanorod array is similar to the one described by Vayssieres[13], who has reported that ZnO nanorods preferred to grow along the c-axis direction. The typical diameters of these individual ZnO nanorods are in the range of 50–200 nm with a length of 600 nm–1.3 μm. The surface of the ZnO hexagonal nanorod is very smooth and well faceted. From the high-magnified FE-SEM image (Fig. 1(f)), it can be seen that ZnO nanorods grown on the TiO_2 film are not so vertical, which may be due to the morphology of the substrate. The nanoporous surface of the TiO_2 film makes the ZnO nanorods grow at various angles to form an interlaced array.

From the series of experiments, we can conclude that the growth time greatly influences the structural shapes of the ZnO

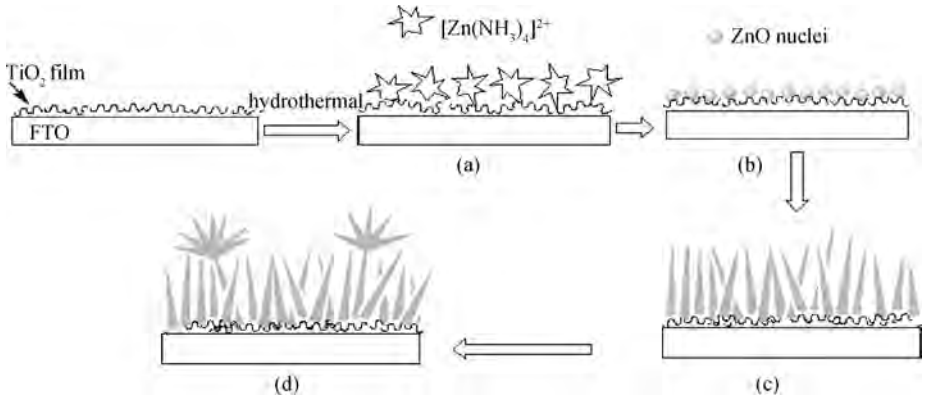

Fig. 3. Schematic growth diagram of the ZnO nano/micro structures on nanoporous TiO_2 films.

grown on the nanoporous TiO_2 film. When the reaction time is less than 1.5 h, only ZnO nanorod arrays grown on the TiO_2 film can be obtained. Two-layer ZnO architectures grown on the TiO_2 film need a reaction time more than 1.5 h.

3.2. Growth mechanism of ZnO architectures on TiO_2 film

Based on the experimental results, the possible formation mechanism of the ZnO architectures on TiO_2 film is proposed. The schematic illustration for the growth mechanism is shown in Fig. 3. Here, at the initial stage of the reaction the growth units ($[Zn(NH_3)_4]^{2+}$)[14] are electrostatically adsorbed onto the surface of the TiO_2 film (Fig. 3(a)), resulting in a decrease in the surface energy and the generation of active sites. Heterogeneous nucleation will take place preferentially at these absorbed sites. With elevated temperature, a large amount of zinc oxide nuclei have formed via the dehydration of abundant component $[Zn(NH_3)_4]^{2+}$ ions reacting with hydroxyl OH^- (Fig. 3(b))[13]. Due to the large quantity of growth units $[Zn(NH_3)_4]^{2+}$ in the solution, anisotropic growth of ZnO is favored and many hexagonal ZnO nanorods growing with *c* axis are formed on the TiO_2 surface in the subsequent stage of growth (Fig. 3(c))[15]. Then, as the ZnO nanorods grow long enough, some of them may contact with each other at the top place due to the different growth angles of the ZnO nanorods. So nanoparticles deposited on these top facets of the ZnO nanorods may serve as the growing nucleus for the second layer. Finally, with the depletion of the precursor and the decrease in growth rate as the reaction time increases, several ZnO nanorods are formed from this nucleation plane in directions of diversity to form the flower-like morphology (Fig. 3(d)).

3.3. X-ray diffraction analysis

The nanoporous TiO_2 film coated on the FTO substrate by the screen-printing method and as-prepared ZnO nano/microstructure hydrothermally grown on the FTO substrate pre-coated with TiO_2 film at different times are characterized by X-ray diffraction. Typical XRD patterns are shown in Fig. 4. As shown in Fig. 4(a), peaks appearing at 25.36°, 37.80°, 48.16°, and 54.06° correspond to (101), (004), (200) and (211) crystal planes of anatase TiO_2 (JCPDS card No 21-1272). No other phases of TiO_2, such as rutile or brookite, can be detected via XRD, indicating that nanoporous TiO_2 film

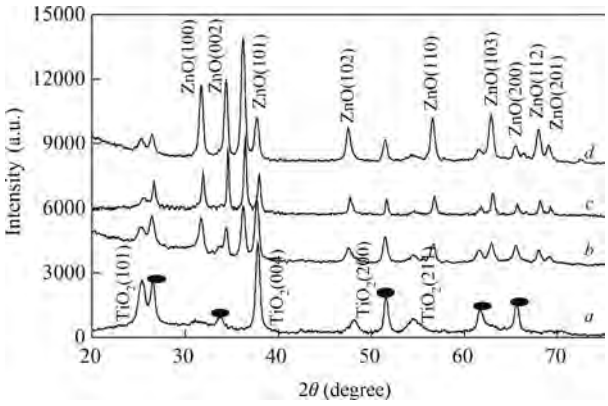

Fig. 4. XRD patterns of (*a*) TiO_2 film on FTO substrate and ZnO architectures synthesized on TiO_2 film for (*b*) 1.5 h, (*c*) 2 h and (*d*) 6 h. The filled circles denote peaks attributed to the FTO substrate.

coated on the FTO substrate is composed of pure anatase-phase TiO_2. Other peaks in Fig. 4(a) correspond to the FTO substrate (filled circles). Figures 4(b)–4(d) show XRD patterns of ZnO structures hydrothermally grown on nanoporous TiO_2 film at 1.5 h, 2 h and 6 h, respectively. Here, except for the peaks of the TiO_2 and FTO substrate, the peaks corresponding to ZnO can be obviously detected. The crystalline peaks with 2θ values of 31.72°, 34.4°, 36.22°, 47.52°, 56.56°, 62.86°, 66.32°, 67.94° and 69.06° in Figs. 4(b)–4(d) are indexed to the hexagonal wurtzite structured ZnO, which is in good agreement with the values in the standard card (JCPDS 36-1451). It is indicated that ZnO structures grown on the TiO_2 film for different times all exhibited the hexagonal wurtzite ZnO.

Moreover, the intensities of the ZnO diffraction peaks increase with the decrease in the intensities of the TiO_2 and FTO peaks as the growth time increases. From the spectrum, it can easily be found that the intensity of the (002) peak increased higher than those of the (100) and (101) peaks. The relative intensity ratio between the (002) and (101) diffraction peaks is usually used to characterize the orientation of the ZnO nanorods[16]. When the growth time increases from 1.5 h to 2 h, the relative intensity ratio has increased from 0.65 to 0.83, indicating that more *c*-textured ZnO nanostructures are formed. However, the relative intensity ratio decreases with the growth time further increasing to 6 h, which may be due to the forma-

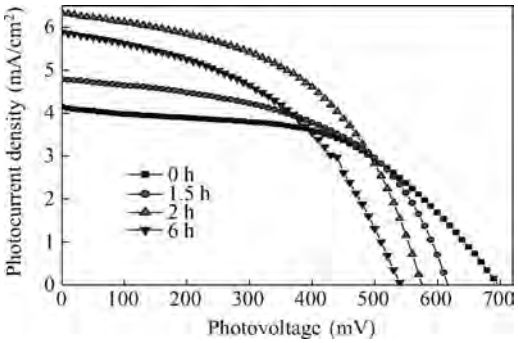

Fig. 5. Photocurrent density–voltage characteristics of the dye-sensitized solar cells with ZnO architecture photoelectrodes grown at 0, 1.5, 2 and 6 h, respectively.

Table 1. Performances of DSSCs with ZnO architecture photoelectrodes grown at 0, 1.5, 2 and 6 h, respectively.

Growth time (h)	V_{oc} (V)	J_{sc} (mA/cm^2)	FF	η (%)
0	0.697	4.135	0.523	1.508
1.5	0.616	4.778	0.526	1.549
2	0.574	6.341	0.506	1.845
6	0.542	5.888	0.461	1.469

tion of many flower-like ZnO structures.

3.4. Current–voltage characteristics

In order to study the photoelectrochemical properties of as-grown ZnO nano/microstructures on the nanoporous TiO_2 film, the photovoltaic parameters of DSSCs containing the synthesized films are tested, in which the ZnO nano/microstructures grown at four different periods of time, i.e., for 0, 1.5, 2 and 6 h. The photocurrent–voltage curves of DSSCs are shown in Fig. 5. The short-circuit photocurrent density (J_{sc}), open-circuit photovoltage (V_{oc}), fill factor (FF) and power conversion efficiency (η) of the DSSCs for ZnO microstructure electrodes of different growth times at 100 mW/cm^2 illumination are presented in Table 1. J_{sc} is defined as the photocurrent density at zero voltage and V_{oc} is defined as the photovoltage at which the photocurrent becomes zero. The fill factor (FF) of the solar cell can be calculated using the equation $FF = J_{max}V_{max}/J_{sc}V_{oc}$ based on the J–V curve, where J_{max} and V_{max} are the photocurrent density and photovoltage for maximum power output. The power conversion efficiency (η) is calculated from the equation $\eta = 100\ (J_{max}V_{max})/P_{in}$, where P_{in} is the power of the incident light.

As seen from Fig. 5 and Table 1, as compared with the DSSC based on TiO_2 substrate film, the J_{sc} values of DSSC based ZnO structures on TiO_2 film have greatly improved. However, the V_{oc} values of DSSCs are lower than that of the TiO_2 cell. The increase in J_{sc} shown by the ZnO-based cell may be due to the increased amount of dye-loading on the ZnO/TiO_2 film. Firstly, ZnO nano/microstructures grown on the TiO_2 substrate result in an increase in the thickness of the electrode, which can effectively increase the dye-absorbed amount. Secondly, the increase in dye-loading amount may also be caused by its novel structure. Although for ZnO electrode the acidic dye-loading solution may dissolve the surface of ZnO, generating Zn^{2+}/dye aggregates, this problem can be greatly released by using a novel structure ZnO electrode. Fujihara[17] has reported that macropores present in the microstructure-controlled ZnO electrodes are effective to release such Zn^{2+}/dye aggregates and increase the amount of dye-loading. In our study, the nanoporous surface of TiO_2 film makes ZnO nanorods grow at various angles to form an interlaced array. An interlaced array or flower-like ZnO microstructure can absorb the significant amount of dye molecules in contrast to the planar structure of ZnO[14]. So, increased dye-loading amounts of electrodes have resulted in an increase in J_{sc}. Moreover, in this novel ZnO microstructure, a ZnO nanorod grown on the bottom layer is a single crystal that can provide an efficient electron transportation channel to the nanoporous TiO_2 film on the conducting substrate[18]. Effective electron transportation ensures a high J_{sc} value of the DSSCs. The decreased V_{oc} values of the DSSCs may be due to the thickness of the ZnO nano/microstructures on the TiO_2 film. From FE-SEM images, it can be seen that ZnO nano/microstructures completely cover the surface of the TiO_2 film when the growth time is more than 1.5 h. Moreover, with the increase in growth time, the ZnO nano/microstructures become thicker and thicker, and the influence of the TiO_2 substrate on the V_{oc}value of the DSSC is reduced, which decreases the V_{oc} value. From Table 1, it can be seen that the fill factors of the DSSCs calculated from the J–V curves have changed very little. As a result of the changes in J_{sc} and V_{oc}, the power conversion efficiency (η) of the corresponding DSSC is increased firstly and then decreased with the increase in growth time. The DSSC based on the composite film grown at 2 h shows better performance ($V_{oc} = 0.574$ V, $J_{sc} = 6.341$ mA/cm^2, FF $= 0.506$ and $\eta = 1.845\%$) than other DSSCs.

From Fig. 5 and Table 1, it can be seen that the performances of the DSSCs based on ZnO structures on TiO_2 film are greatly influenced by the growth time. The performance of DSSC (2 h) is better than that of DSSC (1.5 h) due to its novel two-layer structure. However, the performance of DSSC (6 h) is worse than that of DSSC (2 h). The reason may be related to the amount and size of ZnO architectures. The increased amount and size of ZnO architectures obviously decreases the surface area of the electrode and increases the charge recombination during electron transportation.

4. Conclusions

In summary, a ZnO two-layer architecture, with flower-like microstructure on the top layer and nanorod arrays on the bottom layer, has been successfully synthesized on fluorine-doped SnO_2 (FTO) conducting glass pre-coated with nanoporous TiO_2 film by a one-step hydrothermal process at the very low temperature of 70 ℃. The shape evolution with reaction time is investigated, and a possible growth mechanism is discussed. The results show that the growth time greatly affects the morphology of the obtained ZnO architecture. And a ZnO two-layer architecture only can be formed at a growth time of more than 1.5 h under the present experimental conditions. The dye-sensitized solar cells (DSSCs) are assembled with as-prepared composite film electrodes sensitized by N3 dye, LiI/I_2 electrolyte and a platinum flake counter electrode. It is found that the DSSC based on the composite film grown at 2 h shows better performance than other DSSCs. The rea-

son may be that flower-like ZnO microstructures on the top layer with a proper amount and size could absorb the significant amount of dye molecules in contrast to its planar structure. And ZnO nanorods grown on the bottom layer can provide efficient electron transportation channels to the nanoporous TiO_2 film on the conducting substrate.

References

[1] Zhu B L, Xie C S, Wanb A H, et al. The gas-sensing properties of thick film based on tetrapod-shaped ZnO nanopowders. Mater Lett, 2005, 59(8/9): 1004

[2] Gao X D, Li X M, Yu W D. Flowerlike ZnO nanostructures via hexamethylenetetramine-assisted thermolysis of zinc-ethylenediamine complex. J Phys Chem B, 2005, 109(3): 1155

[3] Han X, Wang G, Jie J, et al. Controllable synthesis and optical properties of novel ZnO cone arrays via vapor transport at low temperature. J Phys Chem B, 2005, 109(7): 2733

[4] Jiang Y H, Sun Y M, Liu H, et al. Solar photocatalytic decolorization of C.I. basic blue 41 in an aqueous suspension of TiO_2/ZnO. Dyes and Pigments, 2008, 78(1): 77

[5] Gao Y F, Nagai M. Morphology evolution of ZnO thin films from aqueous solutions and their application to solar cells. Langmuir, 2006, 22(8): 3936

[6] Law M, Greene L, Johnson J C, et al. Nanowire dye-sensitized solar cells. Nature Mater, 2005, 4: 455

[7] Mane R S, Lee W J, Pathan H M, et al. Nanocrystalline TiO_2/ZnO thin films: fabrication and application to dye-sensitized solar cells. J Phys Chem B, 2005, 109: 24254

[8] Chen J, Chen L, Song J L, et al. Bilayer ZnO nanostructure fabricated by chemical bath and its application in quantum dot sensitized solar cell. Appl Surf Sci, 2009, 255: 7508

[9] Jiang C Y, Sun X W, Lo G Q, et al. Improved dye-sensitized solar cells with a ZnO-nanoflower photoanode. Appl Phys Lett, 2007, 90(26): 263501

[10] O'Regan B, Grátzel M. A low-cost, high-efficiency solar cell based on dye-sensitized colloidal TiO_2 films. Nature, 1991, 353(24): 737

[11] Amao Y, Komori T. Dye-sensitized solar cell using a TiO_2 nanocrystalline film electrode modified by an aluminum phthalocyanine and myristic acid coadsorption layer. Langmuir, 2003, 19: 8872

[12] Shankar K, Bandara J, Paulose M, et al. Highly efficient solar cells using TiO_2 nanotube arrays sensitized with a donor-antenna dye. Nano Letter, 2008, 8: 1654

[13] Vayssieres L. Growth of arrayed nanorods and nanowires of ZnO from aqueous solutions. Adv Mater, 2003, 15(5): 464

[14] Jiang Y H, Wu M, Wu X J, et al. Low-temperature hydrothermal synthesis of flower-like ZnO microstructure and nanorod array on nanoporous TiO_2 film. Mater Lett, 2009, 63(2): 275

[15] Zhai H J, Wu W H, Lu F, et al. Effects of ammonia and cetyltrimethylammonium bromide (CTAB) on morphologies of ZnO nano- and micromaterials under solvothermal process. Mater Chem Phys, 2008,112(3): 1024

[16] Yang L L, Zhao Q X, Willander M. Size-controlled growth of well-aligned ZnO nanorod arrays with two-step chemical bath deposition method. Journal of Alloys and Compounds, 2009, 469(1/2): 623

[17] Kakiuchi K, Saito M, Fujihara S. Growth of high quality rutile TiO_2 thin film using ZnO buffer layer on Si(100) substrate. Thin Solid Films, 2008, 516(8): 2026

[18] Mane R S, Lee W J, Lokhande C D, et al. Controlled repeated chemical growth of ZnO films for dye-sensitized solar cells. Current Applied Physics, 2008, 8(5): 549